Optimal Choice for Number of Strands in a Litz-Wire Transformer Winding

C. R. Sullivan

Found in *IEEE Power Electronics Specialists Conference,* June 1997, pp. 28–35.

Optimal Choice for Number of Strands in a Litz-Wire Transformer Winding

Charles R. Sullivan
Thayer School of Engineering, Dartmouth College, Hanover, NH 03755-8000
chrs@dartmouth.edu http://engineering.dartmouth.edu/inductor

Abstract— **The number of strands to minimize loss in a litz-wire transformer winding is determined. With fine stranding, the ac resistance factor decreases, but dc resistance increases because insulation occupies more of the window area. A power law to model insulation thickness is combined with standard analysis of proximity-effect losses.**

I. Introduction

A salient difficulty in designing high-frequency inductors and transformers is eddy-current effects in windings. These effects include skin-effect losses and proximity-effect losses. Both effects can be controlled by the use of conductors made up of multiple, individually insulated strands, twisted or woven together. Sometimes the term *litz wire* is reserved for conductors constructed according to a carefully prescribed pattern, and strands simply twisted together are called bunched wire. We will use the term *litz wire* for any insulated grouped strands, but will discuss the effect of different constructions.

This paper addresses the choice of the degree of stranding in litz wire for a transformer winding. The number of turns and the winding cross-sectional area are assumed to be fixed. The maximum cross-sectional area of each turn is thus fixed, and as the number of strands is increased, the cross-sectional area of each strand must be decreased. This typically leads to a reduction in eddy-current losses. However, as the number of strands increases, the fraction of the window area that is filled with copper decreases and the fraction filled with insulation increases. This results in an increase in dc resistance. Eventually, the eddy-current losses are made small enough that the increasing dc resistance offsets any further improvements in eddy-current loss, and the losses start to increase. Thus, there is an optimal number of strands that results in minimum loss. This paper presents a method of finding that optimum, using standard methods of estimating the eddy-current losses.

Optimizations on magnetics design may be done to minimize volume, loss, cost, weight, temperature rise, or some combination of these factors. For example, in the design of magnetic components for a solar-powered race vehicle [1] (the original impetus for this work) an optimal compromise between loss and weight is important. Although we will explicitly minimize only winding loss, the results are compatible with and useful for any minimization of total loss (including core loss), temperature rise, volume or weight. This is because the only design change considered is a change in the degree of stranding, preserving the overall diameter per turn and overall window area usage. This does not affect core loss or volume, and has only a negligible effect on weight. However, the degree of stranding does significantly affect cost. Although we have not attempted to quantify or optimize this, additional results presented in Section V are useful for cost-constrained designs.

The analysis of eddy-current losses used here does not differ substantially from previous work [2, 3, 4, 5, 6, 7, 8, 9, 10, 11, 12, 13] ([10] gives a useful review). Although different descriptions can be used, most calculations are fundamentally equivalent to one of three analyses. The most rigorous approach uses an exact calculation of losses in a cylindrical conductor with a known current, subjected to a uniform external field, combined with an expression for the field as a function of one-dimensional position in the winding area [12]. Perhaps the most commonly cited analysis [11] uses "equivalent" rectangular conductors to approximate round wires, and then proceeds with an exact one-dimensional solution. Finally, one may use only the first terms of a series expansion of these solutions, e.g. [9].

All of these methods give similar results for strands that are small compared to the skin depth [12]. (See Appendix B for a discussion of one minor discrepancy.) The solutions for optimal stranding result in strand diameters much smaller than a skin depth. In this region the distinctions between the various methods evaporate, and the simplest analysis is adequate. More rigorous analysis (e.g. [12]) is important when strands are not small compared to a skin depth. In this case, losses are reduced relative to what is predicted by the analysis used here, due to the self-shielding effect of the conductor.

Previous work, such as [2, 3, 4] has addressed optimal wire diameter for single-strand windings. The approach in [2, 3, 4] is also applicable for litz-wire windings in the case that the number of strands is fixed, and the strand diameter for lowest loss is desired. As discussed in Section V, this can be use-

0-7803-3843-X/97/$10.00 (c) 1997 IEEE

ful for cost-sensitive applications, if the number of strands is the determining factor in cost, and the maximum cost is constrained. However, this will, in general, lead to higher-loss designs than are possible using the optimal number of strands.

II. Skin Effect, Proximity Effect, and Litz Wire

Skin effect is the tendency for high-frequency currents to flow on the surface of a conductor. Proximity effect is the tendency for current to flow in other undesirable patterns—loops or concentrated distributions—due to the presence of magnetic fields generated by nearby conductors. In transformers and inductors, proximity-effect losses typically dominate over skin-effect losses. In litz-wire windings, proximity effect may be further divided into internal proximity effect (the effect of other currents within the bundle) and external proximity effect (the effect of current in other bundles) [14, 15]. However, the distinction is useful only as a form of bookkeeping. The actual losses in one strand of a litz bundle are simply a result of the total external field, due to the currents in all the other strands present. Another approach to calculating the loss in a litz winding is to look at it as a single winding, made up of nN turns of the strand wire, each with current i/n flowing in it, where n is the number of strands, N is the number of turns of litz wire, and i is current flowing in the overall litz bundle. The loss in the litz winding will be the same as in the equivalent single-strand winding as long as the currents flowing in all the strands are equal [16]. Other methods of calculating loss in litz wire also assume equal current in all strands [14, 12, 17].

The objective of twisting or weaving litz wire, as opposed to just grouping fine conductors together, is to ensure that the strand currents are equal. Simple twisted bunched-conductor wire can accomplish this adequately in situations where proximity effect would be the only significant problem with solid wire. Where skin effect would also be a problem, more complex litz constructions can be used to ensure equal strand currents. Thus, in a well-designed construction, strand currents are very close to equal. However, our results remain valid even when simple twisting results in significant skin effect at the litz-bundle level. This is because the the bundle-level skin-effect loss is independent of the number of strands, and is orthogonal [15] to the strand-level eddy-current losses.

We represent winding losses by

$$P_{loss} = F_r I_{ac}^2 R_{dc}, \tag{1}$$

where F_r is a factor relating dc resistance to an ac resistance which accounts for all winding losses, given a sinusoidal current with rms amplitude I_{ac}. As shown in Appendix A, we can approximate F_r by

$$F_r = 1 + \frac{\pi^2 \omega^2 \mu_0^2 N^2 n^2 d_c^6 k}{768 \rho_c b_c^2} \tag{2}$$

where ω is the radian frequency of a sinusoidal current, n is the number of strands, N is the number of turns, d_c is the diameter of the copper in each strand, ρ_c is the resistivity of the copper conductor, b_c is the breadth of the window area of the core, and k is a factor accounting for field distribution in multi-winding transformers, normally equal to one (see Appendix A). For waveforms with a dc component, and for some non-sinusoidal waveforms, it is possible to derive a single equivalent frequency that may be used in this analysis (Appendix C). In an inductor, the field in the winding area depends on the gapping configuration, and this analysis is not directly applicable.

The analysis described here considers the strands of all litz bundles to be uniformly distributed in the window, as they would be in a single winding using Nn turns of wire the diameter of the litz strands. In fact, the strands are arranged in more or less circular bundles. In this sense, the analysis of [15] may be more accurate, but this difference has very little effect on the results. The most important difference between the model used here and the model in [15] is the greater accuracy of [15] for strands that are large compared to a skin depth. The simpler model is used because it is accurate for the small strand diameters that are found to be optimal, and because its simplicity facilitates finding those optimal diameters. Other models (such as [14] and the similar analysis in [17]) also model large strand diameters and circular bundle configurations accurately, but they fully calculate only internal, and not external, proximity effect, and so are not useful for the present purposes.

III. DC Resistance Factors

The fraction of the window area occupied by copper in a litz-wire winding will be less than it could be with a solid-wire winding. This leads to higher dc resistance than that of a solid wire of the same outside diameter. A cross section of litz wire is shown in Fig. 1, with the various contributions to cross sectional area marked. In addition to the factors shown in this diagram, the twist of the litz wire also increases the dc resistance. In order to find the optimal number of strands for a litz winding, it is necessary to quantify how the factors affecting dc resistance vary as a function of the number of strands.

Serving

Typically litz bundles are wrapped with textile to protect the thin insulation of the individual strands. This serving adds about 0.06 mm (2.5 mil) to the diameter of the bundle. For a given number of turns filling a bobbin, or a section of a bobbin, the outside diameter of the litz wire must be fixed. The area devoted to serving will then also be fixed, independent of the number of strands.

Strand packing

Simply twisted litz wire comprises a group of strands bunched and twisted into a bundle. More complex constructions begin with this step, and

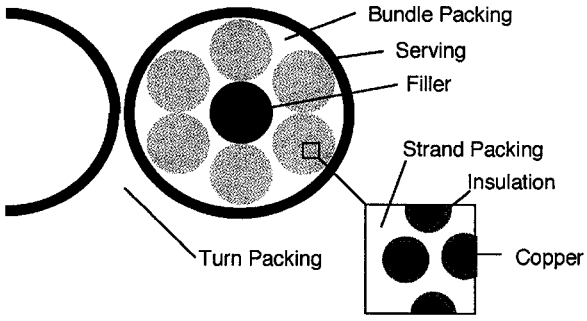

Fig. 1. Cross sectional area of a litz-wire winding, showing how area is allocated. Area allocated to anything other than copper increases the resistance in a space-limited winding.

then proceed with grouping and twisting the sub-bundles into higher-level bundles. Particular numbers of strands (one, seven, nineteen, thirty-seven, etc.) pack neatly into concentric circular arrangements. However, with large numbers of strands (e.g., > 19), and/or very fine strands (e.g., 44-50 AWG), it is difficult to precisely control the configuration, and the practical packing factor becomes an average number relatively independent of the number of strands. Since the optimal strand diameter is typically much smaller than a skin depth, but the lowest-level bundle can be near a skin depth in diameter, in most cases we can assume that there is a large number of strands in the innermost bundle. Thus, this packing factor is independent of the number of strands.

Bundle packing and filler

The way the strands are divided into bundles and sub-bundles is chosen based on considerations including skin-effect losses, flexibility of the overall bundle, resistance to unraveling, and packing density. In some cases, a nonconducting filler material may be used in the center of a bundle in place of a wire or wire bundle that would, in that position, carry no current because of skin effect.

A typical configuration chosen to avoid significant skin-effect losses should have a carefully designed and potentially complex construction at the large-scale level where bundle diameters are large compared to a skin depth. However, because the optimal strand diameter will be small compared to a skin depth, a simple many-strand twisted bundle may be used at the lowest level. If the overall number of strands is increased, the number of strands in each of these low-level bundles should be increased, but the diameter of each low-level bundle should not be changed, nor should the way they are combined into the higher-level construction be affected. Thus, for our purposes, the bundle packing factor is independent of the number of strands.

Turn packing

The way turns are packed into the overall winding is primarily a function of winding technique, and it is assumed not to vary as a function of the stranding. However, note that loosely twisted litz wires can deform as the winding is constructed, allowing tighter packing. Another option providing tight turn packing is rectangular-cross-section litz wire. In addition to its turn-packing advantage, it has tighter strand and bundle packing, as a result of the mechanical compacting process that forms it into a rectangular cross section.

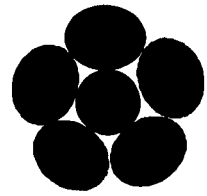

Fig. 2. The cross section of strands becomes elliptical when the bundle is twisted. In this extreme case of lay (length per twist) equal to 4.7 times the bundle diameter, a total of six strands fit where seven would have fit, untwisted.

Twist

The distance traveled by a strand is greater in a twisted bundle than it would be if the strands simply went straight, and so the resistance is greater. An additional effect arises from the fact that a cross section perpendicular to the bundle cuts slightly obliquely across each strand. Thus, the cross section of each strand is slightly elliptical. This reduces the number of strands that fit in a given area, and so effectively increases the resistance. An extreme case of this is illustrated in Fig. 2. The choice of the pitch of the twist ('lay', or length per twist) is not ordinarily affected by the number of strands in the lowest-level bundle, and so, for the purpose of finding the optimal number of strands, we can again assume it is constant.

Strand insulation area

Thinner magnet wire has thinner insulation. However, the thickness of the insulation is not in direct proportion to the wire diameter. Thinner wire has copper in a smaller fraction of the overall cross sectional area, and insulation in a larger fraction.

Of all of the dc-resistance factors considered, this is the only one that varies with the size or number of strands used at the lowest level of the construction. Thus, quantifying this effect on dc resistance gives a good approximation of the total variation in dc resistance as a function of the size or number of strands. The other factors can be lumped into an overall dc resistance multiplying factor which is a constant for the present purposes.

One approach to quantifying the relationship between the insulation area and strand diameter would be to store tables in computers, and use them to find the optimal strand diameter by calculating the losses for different strand diameters until the optimum was found, similar to [6]. However, an analytical description of the variation of insulation thickness with wire

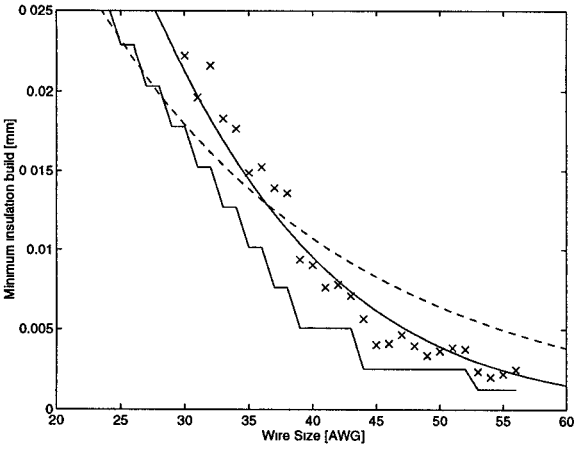

Fig. 3. Insulation build (twice the insulation thickness) for American Wire Gauge (AWG) single-build magnet wire. The dashed curve is the minimum build according to the equation provided by [18]. The lower 'staircase' curve is the tabulated data provided by [18] for minimum build. The points marked by 'x' are nominal build from a wire manufacturer's catalog, obtained by subtracting tabulated nominal overall diameter and subtracting the exact theoretical nominal wire diameter. The approximation described by (4) comes closest to these points.

size can facilitate an analytical solution for the optimal number of strands.

An equation describing magnet wire insulation thickness is provided by [18]:

$$\log_{10} B = X - \frac{AWG}{44.8} \tag{3}$$

where B is the minimum insulation build in mils (10^{-3} in, 1 mil = 25.4 μm), $X = 0.518$ for single-build insulation and $X = 0.818$ for heavy (double) build, and AWG is the American Wire Gauge number [1]. However, this only applies to wire sizes between 14 and about 30 AWG. For smaller wire sizes, it does not correlate with the tabulated data in [18](Fig. 3). For wire in the range of 30 to 60 AWG, we find a better fit to manufacturers' tabulated nominal insulation build by using

$$d_t = d_r \alpha \left(\frac{d_c}{d_r}\right)^{\beta} \tag{4}$$

where d_t is the overall diameter, including the insulation thickness, d_c is the diameter of the copper only, and d_r is an arbitrarily defined reference diameter, used to make the constants α and β unitless. The parameters used for single-build insulation wire were $\beta = 0.97$ and $\alpha = 1.12$ for d_r chosen to be the diameter of AWG 40 wire (0.079 mm). For heavy-build insulation, $\beta = 0.94$ and $\alpha = 1.24$. Note that although (4) provides an accurate approximation for wire in the range of 30 to 60 AWG, its asymptotic behavior for large strand diameters is pathological. Insulation thickness goes to zero around 6 AWG, and is negative for larger strands.

[1]The American wire gauge defines nominal wire diameter in inches as $d = 0.0050(92)^{(36-AWG)/39}$.

IV. Number of Strands for Minimum Loss

For a full bobbin, the outside diameter of the complete litz bundle is,

$$d_{tl} = \sqrt{\frac{F_p b_b h}{N}}, \tag{5}$$

where b_b is the breadth of the bobbin, h is the height allocated for the particular winding under consideration, N is the number of turns in that winding, and F_p is a turn-packing factor for turns in the winding, expressed relative to perfect square packing (For $F_p = 1$, the litz bundle would occupy $\pi/4$ of the window area).

Assuming a factor F_{lp} accounting for serving area, bundle packing, any filler area, strand packing, and the effect of twist on diameter, we can find the outside diameter of a single strand

$$d_t = \sqrt{\frac{F_p F_{lp} b_b h}{nN}}, \tag{6}$$

where n is the number of strands in the overall litz bundle.

The diameter of the copper in a single strand can then be written using (4).

$$d_c = d_r^{1-1/\beta} \alpha^{1/\beta} \left(\frac{F_p F_{lp} b_b h}{nN}\right)^{1/(2\beta)}. \tag{7}$$

We now define a total resistance factor F_r',

$$F_r' = F_{dc} F_r = \frac{\text{ac resistance of litz-wire winding}}{\text{dc resistance of single-strand winding}}, \tag{8}$$

where F_{dc} is the ratio of dc resistance of the litz wire to the dc resistance of a single strand winding, using wire with the same diameter as the litz-wire bundle. Using (6) and (7), we can show

$$F_{dc} = n^{1/\beta - 1} F_{lp}^{-1/\beta} \tag{9}$$

Combining (2), (8), and (9) results in

$$F_r' = F_{lp}^{1/\beta} \left[n^{1/\beta - 1} + \gamma n^{(1-2/\beta)}\right], \tag{10}$$

where

$$\gamma = \frac{\pi^2 N^2 \omega^2 \mu_0^2 d_r^{6-6/\beta} \alpha^{-6/\beta} (F_p F_{lp} b_b h/N)^{3/\beta} k}{768 \rho_c^2 b_c^2} \tag{11}$$

Equation (10) can now be minimized with respect to n to find the optimal number of strands.

$$n_{opt} = \left(\frac{(2/\beta - 1)\gamma}{1/\beta - 1}\right)^{1/(3/\beta - 2)} \tag{12}$$

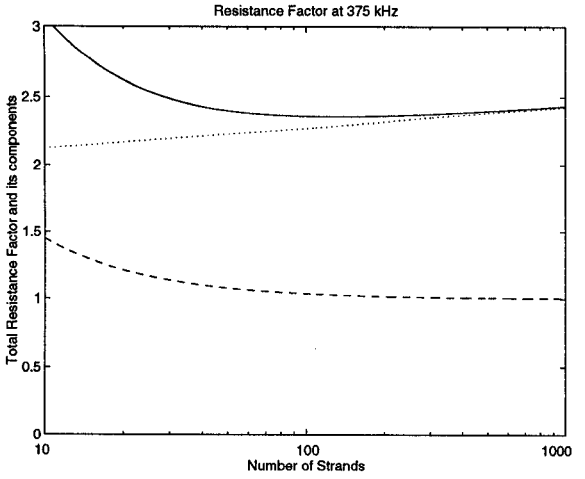

Fig. 4. Total resistance factor, F_r', as a function of number of strands (solid line) for the example discussed in the text at 375 kHz. Also shown are the ac resistance factor F_r (dashed) and the dc resistance factor F_{dc} (dotted). The minimum total resistance factor is at the point where increases in F_{dc} balance decreases in F_r with increasing number of strands.

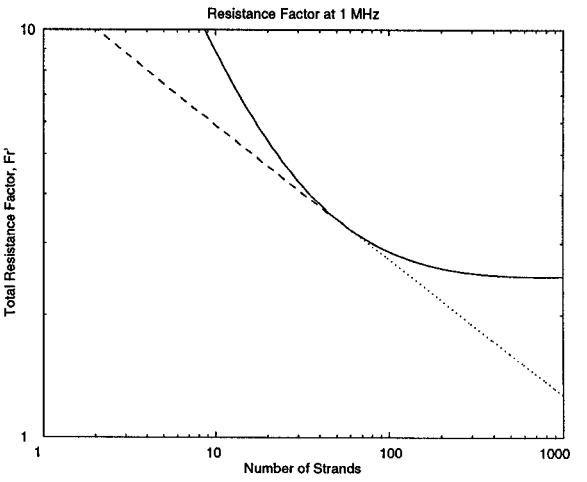

Fig. 5. Total resistance factor, F_r', as a function of number of strands for the example discussed in the text at 1 MHz. The solid line indicates resistance factor for a full bobbin. The dashed line shows the lower resistance that is possible by choosing the strand diameter for minimum loss, with the number of strands fixed. Where this optimal diameter results in a full bobbin, the two curves are tangent. For larger numbers of strands, the optimal strand diameter, shown as a dotted line, would over-fill the bobbin, and so is not possible.

This will give non-integral numbers of strands; the nearest integral number of strands can be chosen to minimize ac resistance.

V. Design Examples and Sub-Optimal Stranding

For a design example, we used a 14-turn winding on an RM5 size ferrite core. The breadth of the bobbin is 4.93 mm, and the breadth of the core window 6.3 mm. A height of 1.09 mm is allocated to this winding. Based on an experimental hand-wound packing factor $F_p = 0.85$, and litz packing factor $F_{lp} = 0.66$, unserved, plus a 32 μm (1.25 mil) thick layer of serving, the above calculation indicates that, for a frequency of 375 kHz, 130 strands of number 48 wire gives minimum ac resistance, with a total resistance factor of $F_r' = 2.35$, ac resistance factor $F_r = 1.03$, and a dc resistance factor $F_{dc} = 2.29$.

Fig. 4 shows the total calculated resistance factor and its components as a function of number of strands. The figure and the numbers confirm the intuition that, because β is close to one and the dc resistance increases only very slowly, the decrease in resistance using finer strands outweighs the decreased cross sectional area until the ac resistance factor is brought very close to one. Note that although the factor F_{dc} is large, only a factor of 1.18 is due to the change in wire insulation thickness. The remaining factor of 1.95 is due to the the dc resistance factors that do not vary with number of strands, such as serving area and strand packing.

The optimization leads to choosing a large number of fine strands, which will often mean a high cost, and will sometimes require finer strands than are commercially available. From Fig. 4, one can see that a decrease from the optimum of 130 to about 50 strands entails only a small increase in ac resistance. Consideration of the cost trade-off for a particular application becomes necessary.

Given a sub-optimal number of strands, chosen to reduce costs, a full bobbin may no longer be best. The problem of choosing the optimal strand diameter for a fixed number of strands has been addressed by many authors, though usually just for a single strand [2, 3, 4, 9]. This analysis can be adapted for more than one strand by simply using the product of the number of turns and the number of strands Nn in place of the number of turns N. The result that $F_{r\,opt} = 1.5$ [2, 3, 4, 9] holds, and

$$d_{opt} = \left(\frac{384 \rho_c^2 b_c^2}{\pi^2 \omega^2 \mu_0^2 N^2 n^2} \right)^{1/6} . \qquad (13)$$

In many practical cases, cost is a stronger function of the number of strands than of the diameter of the strands. In the range of about 42-46 AWG the additional manufacturing cost of smaller wire approximately offsets the reduced material cost. Thus, designs using the diameter given by (13) often approximate the minimum ac resistance for a given cost.

Fig. 5 shows total resistance factor as a function of the number of strands for the same example design, but at 1 MHz, where the optimal stranding is a difficult and expensive 792 strands of AWG 56 wire, and so analysis of alternatives is more important. The solid line is for a full bobbin, and the dashed line is for the same number of strands, but with the diameter chosen for minimum losses, rather than to fill the bobbin. Where the two lines meet, the optimal

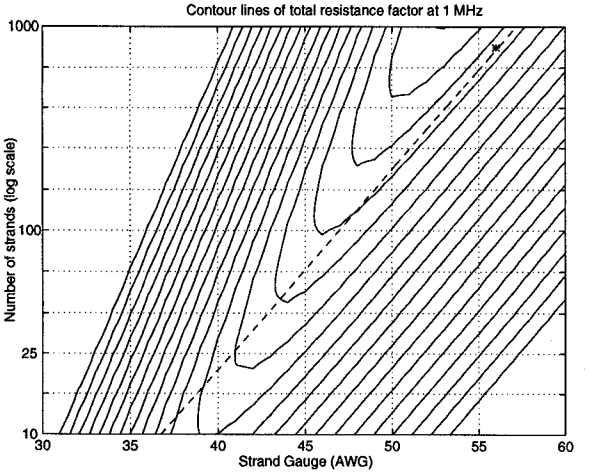

Fig. 6. Contour lines of total resistance factor, F_r', as a function of number of strands and diameter of strands, for the example discussed in the text at 1 MHz. The diagonal dashed line indicates a full bobbin. The valley at the upper right is the minimum loss. The minimum loss without over-filling the bobbin is marked by an 'x'. Contour lines are logarithmically spaced.

diameter just fills the bobbin. Beyond that point it would not fit, and the line is shown dotted.

The example can be understood more completely by examining contour lines of total resistance factor F_r' as a function of both strand diameter and number of strands (Fig. 6). The minimum resistance is in the valley at the upper right (a large number of fine strands). To fit on the bobbin, designs must be below the dashed diagonal line. Minimum loss designs for a fixed number of strands can be found by drawing a horizontal line for the desired number of strands, and finding the point tangent to contour lines.

One could also consider a constraint for minimum wire diameter. Many manufacturers cannot provide litz wire using strands finer than 48 or 50 AWG. On Fig. 6, the minimum resistance for 50 AWG stranding is with a full bobbin, but for 40 AWG wire, the minimum ac resistance can be seen to occur with fewer than the maximum number of strands. This situation can be analyzed by considering (2) with all parameters fixed except for the number of strands, such that

$$F_r = 1 + \zeta n^2 \tag{14}$$

where ζ is a constant obtained by equating (2) and (14). The total resistance factor is then

$$F_r' = F_{dc1} \cdot (1 + \zeta n^2)/n \tag{15}$$

where F_{dc1} is the dc resistance factor with a full bobbin, for the fixed strand diameter. The value of n that minimizes this expression is $n = \sqrt{1/\zeta}$, such that $F_r = 2$. This will be the optimal number of strands, given a fixed minimum strand diameter, unless this is too many strands to fit in the available window area.

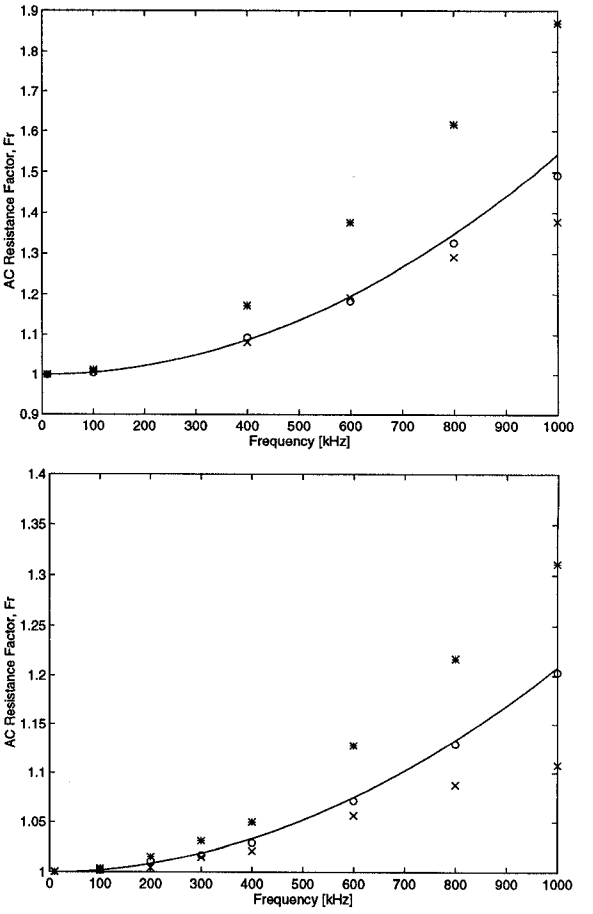

Fig. 7. Experimental ac resistance factor, F_r, as a function of frequency. Top graph is for litz wire with 50 strands of 44 AWG wire; bottom graph is 130 strands of 48 AWG wire. Both are in the example transformer described in the text. Total measured resistance factor in the transformer is marked with stars. Measured skin effect in a straight piece of litz wire is marked with 'x's. The difference, equal to proximity-effect losses, is marked with circles. These correspond closely to the predicted proximity-effect losses (solid line).

VI. Experimental Results

The designs specified in the preceding section were constructed with two types of litz wire: 130 strands of 48 AWG and 50 strands of 44 AWG. The primary and secondary windings were made from a single length of litz wire, wound on the bobbin in opposite directions. This is magnetically equivalent to having a shorted secondary, but it reduces potential problems with interconnect resistance. In order to evaluate skin effect in the absence of external proximity effect litz wire was also measured outside of a winding. The resistance was measured with an HP 4284A LCR meter, using a custom built test jig for low impedance measurements. The measurements are shown in Fig. 7.

Although the overall litz-wire diameter was small enough to limit bundle-level skin-effect losses to a

few percent, the fine strands in the optimal solution also limit proximity-effect losses to similar levels. Fortunately, the losses are orthogonal [15], and the measured skin effect losses (for a litz wire outside of the winding) can be subtracted from the measured losses in the transformer in order to isolate proximity-effect losses. When this is done, the proximity-effect losses predicted by (2) match the measured proximity-effect losses very closely.

Because the exact construction of one of the samples was not known, the expected bundle skin effect could not be predicted accurately. However, the 50-strand bundle of 44 AWG wire was believed to be simply twisted. It exhibited considerably lower loss than would be expected on this basis, indicating that there may be some more complex transposition of the strands, even if the manufacturing process did not deliberately introduce this construction. While these effects merit further experiments, the experiments reported here confirm the validity of the model used in our optimization.

VII. Conclusion

The number of strands for a minimum-loss litz-wire winding may be found by evaluating the tradeoff between proximity-effect losses and dc resistance. Of the factors leading to increased dc resistance in a litz-wire winding, only the space allocated to strand insulation varies significantly with the number of strands in a well designed construction. A power law can be used to model insulation thickness in the region of interest. Combining this with standard models for eddy-current loss results in an analytic solution for the optimal number of strands. The simplest model for loss, using only the first terms of a series expansion can be used since good designs use strands that are small compared to a skin depth. Experimental results correlate well with the simple model.

Stranding for minimum loss may lead to many strands of fine wire and thus excessive expense. Minimum loss designs constrained by minimum strand size or maximum number of strands have also been derived.

VIII. Acknowledgments

Thanks to New England Electric Wire Corporation for litz wire samples and to Magnetics Division of Spang and Co. for ferrite core samples.

Appendix

A. Loss Calculation

The expression for F_r used here may be derived by first calculating loss in a conducting cylinder in a uniform field, with the assumption that the field remains constant inside the conductor, equivalent to the assumption that the diameter is small compared to a skin depth. This results in power dissipation P in a wire of length ℓ

$$P = \frac{\pi\omega^2 \ell B^2 d_c^4}{128\rho_c}, \tag{16}$$

where B is the peak flux density. This is equal to the first term of an expansion of the exact Bessel-function solution [19].

Combining this with the assumption of a trapezoidal field distribution results in (2). For configurations in which the field is not zero at one edge of the winding, a factor $k = (1-\varphi^3)/(1-\varphi)^3$ is used to account for the resulting change in losses, where $\varphi = B_{min}/B_{max}$ [9].

B. Comparison with Expansion of Dowell Solution

Equation (2) is similar to the expression for the first terms of a series expansion of the exact one-dimension solution,

$$F_r = 1 + \frac{5p^2-1}{45}\psi^4, \tag{17}$$

where p is the number of layers and ψ is the ratio of effective conductor thickness to skin depth. For a large number of layers (equivalent to the assumption, above, of a trapezoidal field distribution), this reduces to $F_r = 1 + \frac{p^2}{9}\psi^4$. The usual expression for ψ is

$$\psi = \sqrt{F_l}\, h_{eq}/\delta. \tag{18}$$

where $F_l = N_l b_{eq}/b_b$, h_{eq} and b_{eq} are the height and breadth of an "equivalent" rectangular conductor, and N_l is the number of turns per layer. Based on equal cross sectional area, $b_{eq} = h_{eq} = \sqrt{\pi/4}\, d_c$. This results in

$$\psi^4 = \frac{(\pi/4)^3 d_c^6 N n}{\delta^4 b_b h_b}, \tag{19}$$

where h_b is the height of the bobbin area allocated to this winding. The number of layers is $p = \sqrt{nNh_b/b_b}$. Substituting these expressions for p and ψ into the simplified version of (17), and using $\delta = \sqrt{2\rho_c/(\mu_0\omega)}$, we obtain

$$F_r = 1 + \frac{\pi^3\omega^2\mu_0^2 N^2 n^2 d_c^6 k}{3\cdot 768\rho_c b_b^2}, \tag{20}$$

the same as (2), except for the substitution of b_b for b_c, and the addition of a factor of $\pi/3$. This discrepancy can be explained by comparing (16) to the equivalent expression for a rectangular conductor

$$P = \frac{\omega^2 \ell B^2 s^4}{24\rho_c}. \tag{21}$$

where s is the side of a square conductor. Equating these two, we obtain $s = (3\pi/16)^{1/4} d_c$. Thus, it appears that using an equivalent square conductor with sides equal to $s = (3\pi/16)^{1/4} d_c$ would be a more accurate approximation than the equal area approximation that is usually used [11].

C. Non-Sinusoidal Current Waveforms

Non-sinusoidal current waveforms can be treated by Fourier analysis. The current waveform is decomposed into Fourier components, the loss for each component is calculated, and the loss components are summed to get the total loss:

$$P = \sum_{j=0}^{\infty} I_j^2 F_r(\omega_j) R_{dc} \tag{22}$$

where I_j is the rms amplitude of the Fourier component at frequency ω_j. From (2) it can be seen that

$$F_r(\omega) = 1 + (F_R(\omega_1) - 1)\frac{\omega^2}{\omega_1^2}. \quad (23)$$

Defining F_{r-tot} by $P = I_{tot-rms}^2 F_{r-tot} R_{dc}$ leads to

$$F_{r-tot} = 1 + \frac{(F_r(\omega_1) - 1)\sum_{j=0}^{\infty} I_j^2 \frac{\omega_j^2}{\omega_1^2}}{I_{tot-rms}^2} \quad (24)$$

This can also be written as

$$F_{r-rms} = 1 + (F_R(\omega_1) - 1)\frac{\omega_{eff}^2}{\omega_1^2}. \quad (25)$$

where

$$\omega_{eff} = \sqrt{\frac{\sum_{j=0}^{\infty} I_j^2 \omega_j^2}{\sum_{j=0}^{\infty} I_j^2}}. \quad (26)$$

One may calculate this effective frequency for a non-sinusoidal current waveform and use it for analysis of litz-wire losses, or for other eddy-current loss calculations. Note that this applies to waveforms with dc plus sinusoidal or non-sinusoidal ac components. The results will be accurate as long as the skin depth for the highest important frequency is not small compared to the strand diameter.

A triangular current waveform with zero dc component results in an effective frequency of $1.103\omega_1$, where ω_1 is the fundamental frequency. Once the effective frequency of a pure ac waveform has been calculated, the effective frequency with a dc component can be calculated by a re-application of (26):

$$\omega_{eff} = \sqrt{\frac{I_{ac}^2 \omega_{eff-ac}^2}{I_{dc}^2 + I_{ac}^2}}. \quad (27)$$

Finding Fourier coefficients and then summing the infinite series in (26) can be tedious. A shortcut, suggested but not fleshed out in [4], can be derived by noting that

$$\sum_{j=0}^{\infty} I_j^2 \omega_j^2 = \left[RMS\{\frac{d}{dt} I(t)\}\right]^2 \quad (28)$$

so that

$$\omega_{eff} = \frac{RMS\{\frac{d}{dt} I(t)\}}{I_{tot-rms}}. \quad (29)$$

The primary limitation of effective-frequency analysis is that it does not work for waveforms with more substantial harmonic content. For instance, the series in (26) does not converge for a square wave. Similarly, the derivative of a square wave in (29) results in an infinite rms value. A Bessel-function-based description of loss may be necessary. However, in practice leakage inductance prevents an inductive component from having perfectly square current waveforms. A square wave with finite-slope edges leads to a finite value of ω_{eff}. If the skin depth for this effective frequency is not small compared to the strand diameter, the simple analysis of loss in (2) will still give accurate results, and the analysis of litz-wire stranding given here is still accurate.

References

[1] Charles R. Sullivan and Matthew J. Powers. A high-efficiency maximum power point tracker for photovoltaic arrays in a solar-powered race vehicle. In *23rd Annual IEEE Power Electronics Specialists Conference*, 1993.

[2] J. Jongsma. Minimum loss transformer windings for ultrasonic frequencies, part 1: Background and theory. *Phillips Electronics Applications Bulletin*, E.A.B. 35(3):146–163, 1978.

[3] J. Jongsma. Minimum loss transformer windings for ultrasonic frequencies, part 2: Transformer winding design. *Phillips Electronics Applications Bulletin*, E.A.B. 35(4):211–226, 1978.

[4] J. Jongsma. High frequency ferrite power transformer and choke design, part 3: Transformer winding design. Technical Report 207, 1986.

[5] P. S. Venkatraman. Winding eddy current losses in switch mode power transformers due to rectangular wave currents. In *Proceedings of Powercon 11*, pages 1–11. Power Concepts, Inc., 1984.

[6] N. R. Coonrod. Transformer computer design aid for higher frequency switching power supplies. In *IEEE Power Electronics Specialists Conference Record*, pages 257–267, 1984.

[7] J. P. Vandelac and P. Ziogas. A novel approach for minimizing high frequency transformer copper losses. In *IEEE Power Electronics Specialists Conference Record*, pages 355–367, 1987.

[8] Lloyd H. Dixon Jr. Review of basic magnetics. theory, conceptual models, and design equations. In *Unitrode Switching Regulated Power Supply Design Seminar Manual*, pages M4–1 to M4–11. Unitrode Corporation, 1988.

[9] E. C. Snelling. *Soft Ferrites, Properties and Applications*. Butterworths, second edition, 1988.

[10] Audrey M. Urling, Van A. Niemela, Glenn R. Skutt, and Thomas G. Wilson. Characterizing high-frequency effects in transformer windings–a guide to several significant articles. In *APEC 89*, pages 373–385, March 1989.

[11] P.L. Dowell. Effects of eddy currents in transformer windings. *Proceedings of the IEE*, 113(8):1387–1394, August 1966.

[12] J. A. Ferreira. Improved analytical modeling of conductive losses in magnetic components. *IEEE Transactions on Power Electronics*, 9(1):127–31, January 1994.

[13] J. A. Ferreira. *Electromagnetic Modelling of Power Electronic Converters*. Kluwer Academic Publishers, 1989.

[14] A. W. Lotfi and F. C. Lee. A high frequency model for litz wire for switch-mode magnetics. In *Conference Record of the 1993 IEEE Industry Applications Conference Twenty-Eighth IAS Annual Meeting*, volume 2, pages 1169–75, October 1993.

[15] J. A. Ferreira. Analytical computation of ac resistance of round and rectangular litz wire windings. *IEE Proceedings-B Electric Power Applications*, 139(1):21–25, January 1992.

[16] Bruce Carsten. High frequency conductor losses in switchmode magnetics. In *Technical Papers of the First International High Frequency Power Conversion 1986 Conference.*, pages 155–176, May 1986.

[17] Massimo Bartoli, Nicola Noferi, Alberto Reatti, and Marian K. Kazimierczuk. Modeling litz-wire winding losses in high-frequency power inductors. In *27th Annual IEEE Power Electronics Specialists Conference*, volume 2, pages 1690–1696, June 1996.

[18] National Electrical Manufacturer's Association. *Magnet Wire*, MW-1000-1997 edition.

[19] Jiri Lammeraner and Milos Stafl. *Eddy Currents*. CRC Press, 1966. English translation edited by G. A. Toombs.